

Weathering of calcareous bedrocks is strongly affected by the activity of soil microorganisms

Giovanni Pastore^a, Alfons R. Weig^b, Eduardo Vazquez^a, Marie Spohn^{a,c,*}

^a Department of Soil Biogeochemistry, Bayreuth Center of Ecology and Environmental Research (BayCEER), University of Bayreuth, Germany

^b Keylab for Genomics and Bioinformatics, University of Bayreuth, Germany

^c Biogeochemistry of Forest Soils, Swedish University of Agricultural Sciences, Uppsala, Sweden

ARTICLE INFO

Handling Editor: Ingrid Kögel-Knabner

Keywords:

Calcareous soils
Phosphate-solubilizing bacteria
Dolomite
Limestone
Phosphate solubilization
Phosphate adsorption

ABSTRACT

Phosphorus (P) availability in calcareous forest soils is commonly low compared to siliceous soils. The main reason for this is that phosphate ions tend to precipitate with calcium (Ca). Weathering of calcareous rocks and the potential of microorganisms to dissolve calcareous parent material is not fully understood. Therefore, we examined microbial carbonate dissolution and the abundance of phosphorus-solubilizing bacteria in temperate forest soils with contrasting calcareous parent materials. We incubated soil extracts with weathered parent materials (i.e., dolomite and limestone) from two calcareous forest soils differing in P content and determined the rates of P and Ca solubilization. In addition, we determined the abundance of phosphorus-solubilizing bacteria (PSB). We found that the net Ca solubilization rate ranged from 8.8 to 511.1 nmol m⁻² d⁻¹ across both soils and depths. Calcium dissolution rates were negatively related to pH and positively related to the concentration of organic acids. The gross P solubilization rates were on average 63.6% higher from dolomite (P-poor soil) than from limestone (P-rich soil). The abundance of soil PSB ranged from 3.8 % at the limestone site (P-rich soil) to 24.4 % at the dolomite site (P-poor soil). The higher abundance of PSB in the soil derived from dolomite is in line with the high Ca and P solubilization rates at this site, indicating that PSB abundance is related to rock weathering rates from calcareous soils. Pseudomonadales and Enterobacteriales were by far the two most abundant bacterial orders in the PSB community of both soils and soil depths. In conclusion, this study shows, first, that weathering of calcareous bedrocks is strongly affected by the activity of soil microorganisms, and second, that there is likely a selective pressure in P-poor soils towards a higher abundance of PSB.

1. Introduction

Weathering of bedrock is the result of physico-chemical and biological processes that render nutrients available for uptake by organisms (Arvin et al., 2017; Finlay et al., 2019; Zaharescu et al., 2019; Wan et al., 2019). Phosphorus (P) is an essential nutrient and occurs in soils as phosphate ion. Once dissolved in the soil solution, P can be taken up by organisms (Ruttenberg, 2003). The dissolved P concentrations in the soil liquid phase is generally very low (Plante, 2007). The reason for this is that phosphate ions become quickly unavailable through (i) adsorption to soil colloids and (ii) precipitation with cations, depending on the pH conditions of the soil (Lindsay, 1979; Hinsinger, 2001). In alkaline and calcareous soils, P availability is mainly reduced by precipitation of phosphate with calcium (Ca) and magnesium (Mg) ions (Dreybrodt et al., 1996; Kaufmann and Dreybrodt, 2007).

Carbonates constitute up to 15% of the sedimentary rock of the Earth's crust (Fairbridge et al., 1967) and occur in various climatic zones mainly in form of the minerals calcite [CaCO₃] and dolomite [CaMg(CO₃)₂] (Bisutti et al., 2004). Younger carbonates are predominantly limestones (rich in calcite) that when exposed to acidic environments release Ca and carbon dioxide (CO₂). Dolomites react with acids more slowly than limestones and, therefore, their dissolution occurs at a lower rate (Liu et al., 2005). One reason for this is that dolomite may contain significant amounts of detrital silicate minerals which are scantily soluble in water (Taylor et al., 2019). Both limestones and dolomites may contain high P concentrations, ranging from 1.5 to 2.8 g kg⁻¹ due to the apatite minerals they contain (Porder and Ramachandran, 2013). Apatites belong to the group of Ca-phosphates whose solubility increases in the presence of protons (H⁺) in aqueous solutions (Hinsinger, 2001; Bengtsson and Sjöberg, 2009). While the abiotic dissolution of

* Corresponding author at: Biogeochemistry of Forest Soils, Swedish University of Agricultural Sciences, Uppsala, Sweden.

E-mail address: marie.spohn@slu.se (M. Spohn).

<https://doi.org/10.1016/j.geoderma.2021.115408>

Received 9 December 2020; Received in revised form 17 July 2021; Accepted 19 August 2021

Available online 6 September 2021

0016-7061/© 2021 The Authors. Published by Elsevier B.V. This is an open access article under the CC BY license (<http://creativecommons.org/licenses/by/4.0/>).

carbonates has been intensively studied, less is known about the biological contribution to this process.

Soil microorganisms can accelerate the weathering of carbonate rocks and apatite minerals (Banfield et al., 1999; Napieralski et al., 2020). Weathering of carbonates leads to solubilization of Ca, while weathering of apatite leads to solubilization of P. In addition, soil microorganisms can increase the desorption of P and Ca, which is also referred to as solubilization (Hinsinger, 2001). Bacteria with a high capacity to solubilize P are known as P-solubilizing bacteria (PSB). The mechanisms used by soil PSB to convert insoluble P forms into available P forms are acidification and production of chelating compounds (Goldstein, 1995). Microbes can release organic acids and siderophores which can chelate Ca and Mg cations bound to phosphate through their hydroxyl and carboxyl groups, which prevents the cations from precipitating with phosphate (Khan et al., 2009). Organic acids can also contribute to the acidification of the soil solution or can serve as selective ligands (ligand exchange) with elements of similar charge in the crystal lattice (Rodríguez and Fraga, 1999). To the best of our knowledge, only one study investigated the ability and the role of soil PSB collected from calcareous soils in the solubilization of tricalcium phosphate (Liu et al., 2015), and it is currently unknown to what extent microorganisms affect the Ca and P solubilization of calcareous parent materials in temperate forest soils. Thus, the principal aim of this study was to determine Ca and P solubilization rates of two alkaline soils developed on different calcareous parent materials. For this purpose, we incubated weathered limestone and dolomite from two temperate beech forest soils with water extracts of the soils and determined the Ca and P solubilization rate. Organic acids and the pH were quantified at different time points during the incubation. A second objective was to determine to which extent the abundance and the taxonomy of PSB from calcareous forest soils is related to the Ca and P solubilization rates from calcareous parent materials. In this regard, the abundance and the taxonomy of soil PSB was assessed by using a physiological assay in combination with 16S rRNA gene sequencing. First, we hypothesized that the Ca and P solubilization rates from limestone are higher than those from dolomite. Second, we hypothesized that the release of organic acids by microbes is positively correlated with the amounts of Ca released from both calcareous rocks. Third, we hypothesized that the relative abundance of PSB is higher in soils developed on dolomite than on limestone because the relative low P content in dolomite favors bacteria that can mobilize P.

2. Materials and methods

2.1. Study sites and sampling

Soils and weathered calcareous parent materials were sampled in September 2018 from two temperate forest ecosystems (*Fagus sylvatica* L., *Picea abies* L. H. Karst. and *Pseudotsuga menziesii* Mirb. Franco) in Germany. The Tuttlingen site developed on limestone and is located in

proximity to the Swabian Alps (47°59' N, 8°45' E), whereas the site Mangfallgebirge developed on dolomite and is part of the central Bavarian Alps (47°39' N, 11°56' E). The composition of the two parent materials is described in Priezel et al. (2021). The sites are located at 820 and 1190 m above sea level and differ in terms of precipitation and tree species composition (Table 1). The soils of the two study sites are classified as Leptosol as described in Christophel et al. (2013) and Priezel et al. (2016). Some important chemical characteristics of the mineral soil horizons of the two forest soils are shown in Table 2. One profile was excavated at each site, and two different genetic horizons; the AC horizon and the weathered C horizon, were sampled in each profile. The samples were taken in 4–9 and 22–37 cm depth at the dolomitic site and in 11–18 and 42–60 cm depth at the limestone site. In addition, weathered calcareous parent materials were collected from each soil horizon. The pH of the studied soils ranged from 7.2 to 8.6 (Table 2). Field-moist samples were sieved in the laboratory (<2 mm) and all organic debris was removed. From each soil sample one aliquot was air-dried for chemical analyses, another aliquot was stored at 5 °C for the incubation experiments and a third one was frozen at –20 °C for microbial analysis.

2.2. Preparation and characteristics of calcareous parent materials

Weathered calcareous parent materials were crushed using a jaw crusher (Pulverisette, Fritsch, Germany). Each crushed sample was initially sieved through a 0.63 mm sieve. The resulting size fraction was further sieved through a 0.2 mm sieve. The material that did not pass the latter was used for the incubation experiments (0.2–0.63 mm size fraction). The specific surface area (SSA) of each crushed weathered parent material was determined by N₂ adsorption on a micromeritics automatic analyzer (Gemini 2375, Shimadzu, Japan). The adsorption isotherms were evaluated for adsorbent surface area with the BET (Brunauer-Emmet-Teller) model by the instrument software (StarDriver v2.03). In order to analyze the contents of total Ca (TCa) and total P (TP) from parent materials, 100 mg of crushed subsamples were digested using a combination of 2 ml nitric acid (65% HNO₃) and 5 ml hydrochloric acid

Table 2
Chemical characteristics of the mineral soil horizons of the two forest soils at Mangfallgebirge (dolomite) and Tuttlingen (limestone).

Site	Soil depth [cm]	Soil pH [H ₂ O]	Total C [g kg ⁻¹]	Total N [g kg ⁻¹]*	Total P [g kg ⁻¹]	Microbial biomass C [mg g ⁻¹]
Dolomite	4–9	7.3	92.2	6.2	0.6	2.6
	22–37	7.6	48.5	2	0.3	1.4
Limestone	11–18	7.2	46.5	3.8	1	2.9
	42–60	8.6	39.5	–	0.7	0.1

* missing values were below the detection limit (0.5 g kg⁻¹).

Table 1

Basic characteristics of the two forest soils and their weathered calcareous parent material at Mangfallgebirge (dolomite) and Tuttlingen (limestone). Abbreviations: SSA (specific surface area), TP (total phosphorus) and TCa (total calcium).

Site	Forest type	Stand age [yr.]	Elevation [m a. s. L.]	MAT [C]	MAP [mm]	Soil type [WRB 2007]	Soil depth [cm] ^a	SSA of parent material [m ² g ⁻¹]	TP of parent material [mg kg ⁻¹]	TCa of parent material [g kg ⁻¹]
Triassic Dolomite	<i>Fagus sylvatica</i> , <i>Picea abies</i> , <i>Pseudotsuga menziesii</i>	120	1190	5.5	1863	Haplic Leptosol	4–9	3.8	53.1	210
Jurassic Limestone	<i>Fagus Sylvatica</i>	90	820	6.6	855	Rendzic Leptosol	22–37	2.0	43.6	218
							11–18	5.1	382	379
							42–60	3.5	264	387

^a The sampling depths refers to the same genetic horizon (AC and C horizon) in both soils.

(37% HCl) brought to a final volume of 40 ml by adding distilled water. Each sample was digested in three replicates and Ca and P contents were determined by inductively coupled plasma optical emission spectroscopy ICP-OES (Vista-Pro radial, Varian). The specific absorption of radiation for Ca and P was 356 nm and 190 nm, respectively. The reference material used for the analysis consisted of spectrapure standards surface water type 2 for Ca (SPS-SW2) and spectrapure standards waste water type 2 for P (SPS-WW2) (LGC Standards, France).

2.3. Soil chemical analyses

Soil pH of dried samples (60 °C for 24 h) was measured by a SenTix gel electrode (WTW, Xylem Analytics, Germany) in a suspension with deionized water at a ratio of 1:5 (w/v) after an equilibration time of 3 h (Table 2). Sub aliquots of oven dried samples were finely grounded in a ball mill (MM400, Retsch, Germany) and the total soil carbon (TC) and nitrogen (TN) concentrations were determined using a CN elemental analyzer (Vario MAX, Elementar, Germany). Total soil phosphorus (TP) concentrations of dried samples were measured using inductively coupled plasma optical emission spectroscopy (ICP-OES, Vista-Pro radial, Varian) after pressure digestion in concentrated nitric acid.

2.4. Soil microbial biomass

Soil microbial biomass C and N were determined using the chloroform fumigation-extraction method (Brookes et al., 1982; Vance et al., 1987). Briefly, 10 g of fresh soil were split into two equal parts, of which 5 g were fumigated in a desiccator at room temperature for 24 h with ethanol-free CHCl_3 and the other 5 g were used as controls (hereafter referred to as non-fumigated samples). For microbial C and N, fumigated and non-fumigated samples were extracted in 0.5 M K_2SO_4 with a ratio (w/v) of 1:5 (Joergensen, 1996). The C and N contents in the soil extracts were determined with a CN analyzer (multi N/C 2100, Analytik Jena). Soil microbial biomass C and N were calculated as the difference of C and N concentrations in fumigated and non-fumigated samples. Both concentrations were then corrected by a factor of 2.22 (Jenkinson et al., 2004).

2.5. Incubation experiments

To determine the net Ca and P solubilization rates from the weathered calcareous parent materials, incubation experiments were conducted using soil extracts following Brucker et al. (2020) and Pastore et al. (2020a); Pastore et al. (2020b). For this purpose, a soil extract from one soil was incubated with weathered bedrock of the same soil horizon. The soil extracts used for the incubations were prepared as follows: 100 g of each soil sample were placed in PE bottles and mixed with 1 L of distilled water and shaken at room temperature for 2 h using an overhead shaker. The extracts were then filtered through cellulose filters with coarse pores that allow for passage of soil microorganisms and small organic matter particles (Rotilabo, type 113P, Roth, Germany). To determine the Ca and P solubilization rates from calcareous parent materials, three incubation experiments were conducted, all once with and once without the addition of glucose. Glucose was added to soil extracts to provide microbes with a readily available carbon (C) source since it was observed in previous experiments (Pastore et al., 2020a; Pastore et al., 2020b) that the rate of microbial P solubilization is very small, and can only be determined in incubation experiments if microbial activity is stimulated. The glucose addition reflects the situation in the rhizosphere, where a large flux of sugars enters the soil. In experiment 1, the total Ca and P mobilization rates from parent material were determined. For this purpose, 1 g of each parent material was incubated with 99 ml of the respective soil extract and with/without 1 ml of glucose solution (3.33 mM). In experiment 2, we quantified the mobilization of P from the dissolved organic matter in order to determine organic P mineralization, either with or without the addition of glucose.

This experiment was conducted in the same way as experiment 1 but without parent material, thus the only source of P was organic P. Third, sterile control incubations were conducted to determine the chemical effect of the sterile soil extracts on Ca and P solubilization. All experiments were performed in triplicates. The incubation flasks were loosely covered with aluminium foils and continuously agitated at 20 °C for fourteen days on a horizontal shaker.

2.6. Chemical analyses of soil extracts incubated with parent material

In each soil extract, dissolved Ca was measured 0, 3, 7, and 14 days after the beginning of the experiment. Aliquots of 6 ml were taken and filtered through cellulose acetate filters of 0.45- μm pore size (Sartorius Biotech, Germany). The filtrates were acidified by adding 30 μl of 65% HNO_3 to prevent Ca precipitation and then centrifuged at $1500 \times g$ for 15 min. The resulting supernatant was analysed for Ca by ICP-OES (Vista-Pro radial, Varian, USA). In parallel, the amounts of phosphate released from parent materials were also quantified. At defined time intervals (0, 3, 7, 10, and 14 days after the beginning of the experiment), 10 ml were taken from the flasks and vacuum filtered using 0.45 μm cellulose acetate filters. The resulting filtrates were analysed for pH and phosphate concentration. The latter was determined according to the molybdenum-blue assay (Murphy and Riley, 1962) and measured with an Infinite M200 Pro microplate reader (Tecan, Switzerland).

2.7. Organic acids

Organic acids (citric, oxalic, 2-keto-D-gluconic, D-gluconic and lactic) were determined in filtered samples from soil extracts incubated with the respective parent material and glucose on day 7 and 14 after the beginning of the experiment. We chose acids that have been identified as the major organic acids relevant in P solubilization (Rodríguez and Fraga, 1999). All filtrates were examined by means of high-performance liquid chromatography (Agilent series 1200, Germany) coupled to a diode array HPLC detector (DAD). Chromatographic separation of the organic acids was performed with a Rezex™ ROA-Organic Acid H^+ (8%), LC column (300 \times 7.8 mm; Phenomenex) equipped with a matching guard column. Organic acids were identified based on their retention times. The solvent used to separate organic acids consisted of 4 mmol phosphoric acid aqueous solution at a flow rate of 0.8 ml min^{-1} . Quantification was performed according to the external standard calibration method. HPLC-MS data were processed using the Agilent Chemstation software package. The amounts of each organic acid were calculated by multiplying the respective concentration (mg l^{-1}) in the soil extracts by the volume (l) present in the flask at the time of sampling, and subsequently expressed in μmol . The concentrations of the carboxyl groups were determined from the concentrations of organic acids and the respective number of carboxyl groups of each acid (mono-, di- and tri-carboxylic).

2.8. Abundance of PSB

The relative abundance of culturable PSB was assessed by suspending 0.5 g of fresh soil in 49.5 ml of sterile water and shaking for 1 h. Serial dilutions (10^{-3} , 10^{-4}) from each soil suspension were tested to identify the appropriate cell density. Subsequently, from each suspension, an aliquot of 100 μl was spread on Pikovskaya's agar medium (PVK, Pikovskaya, 1948) and the plates were incubated at ~ 20 °C for 7 days. The PVK medium was composed of: 10 g glucose; 5 g hydroxyapatite; 0.5 g yeast extract; 0.5 g ammonium sulphate; 0.2 g potassium chloride; 0.2 g sodium chloride; 0.1 g magnesium sulphate; 0.002 g ferrous sulphate; 0.002 g manganese sulphate and 15 g agar-agar in 1 L distilled water. The pH of the medium was adjusted to 7.0. If a bacterial colony dissolves hydroxyapatite present in the medium, a halo (clear zone) becomes visible in the otherwise milky medium. When bacterial colonies produced halos with a diameter larger than 1 mm, the relative

isolate was classified as “strong” PSB. When the halos had a diameter lower than 1 mm, the relative isolate was classified as “weak” PSB. The relative abundance of culturable PSB was calculated as the percentage of colonies that were formed by PSB of the total number of bacterial colonies.

2.9. Amplification and sequencing of PSB (16S rRNA gene)

Bacterial colonies identified as PSB were collected using sterile toothpicks and aseptically transferred into buffer solutions for sequencing analysis as described in Widdig et al. (2019). Sequence similarity searches of high-quality regions larger than 514 bp were conducted against NCBI’s nucleotide database (Nucleotide [Internet]. Bethesda (MD): National Library of Medicine (US), National Center for Biotechnology Information, available from: <https://www.ncbi.nlm.nih.gov/nucleotide/>) and against the 16S section of NCBI’s RefSeq Targeted Loci Project (RefSeq Targeted Loci Project [Internet]. Bethesda (MD): National Library of Medicine (US), National Center for Biotechnology Information, available from: <https://www.ncbi.nlm.nih.gov/efseq/targetedloci/>) (max e-value 1e-10). Sequence data were processed using Geneious v. 11 (Biomatters Ltd., New Zealand) and aligned using MAFFT software (v. 7.388; see also Katoh and Standley, 2013). The best 20 hits were selected. Sequences with a 98% cut-off similarity were clustered into operational taxonomic units (OTUs). To this end, the name of the lowest common rank in the taxonomy was chosen. Only the non-redundant top hits were selected for taxonomic annotation. For this purpose, each 16S sequence was compared with all other sequences and sequences sharing identity above 98% identity were assigned to one taxon. Major phylogenetic changes were detected at the order and genus levels by means of ANOVA with a false discovery rate correction test (FDR, $p < 0.05$). The partial 16S rRNA gene sequences were deposited in GenBank (<https://www.ncbi.nlm.nih.gov/genbank/>) under the accession numbers MT955367-MT955590. The abundance matrix of the 16S sequence types was uploaded in PRIMER 7 (PRIMER-E Ltd., United Kingdom), standardized and cumulated at the genus level. A resemblance matrix (Manhattan distance) was calculated from the abundance matrix of bacterial fragments before nonmetric multi-dimensional scaling (nMDS) was performed (using a stress test = 0.01). Subsequently, analyses of similarities (ANOSIM) based on the number of OTU grouped by taxon were conducted using 999 permutations to determine whether the P-solubilizing bacterial communities were significantly different among the tested soils.

$$\text{GrossPsolubilizationrate}(\text{nmold}^{-1}) = \frac{\text{NetCasolubilizationrate}[\text{nmold}^{-1}] * \text{Pcontent}[\text{gKg}^{-1}]}{\text{Cacontent}[\text{gkg}^{-1}]} \quad (3)$$

2.10. Data analyses and statistics

The amounts of Ca and P in the incubated soil extracts were calculated by multiplying the element concentration (nmol l^{-1}) with the volume (l) of the soil extract at the time of sampling. The total Ca mobilization rates represent the change in the amounts of Ca from the parent material in the solution over fourteen days (biotic + abiotic) and were computed according to the following equation (Eq. (1)).

2.10. Data analyses and statistics

The amounts of Ca and P in the incubated soil extracts were calculated by multiplying the element concentration (nmol l^{-1}) with the volume (l) of the soil extract at the time of sampling. The total Ca mobilization rates represent the change in the amounts of Ca from the parent material in the solution over fourteen days (biotic + abiotic) and were computed according to the following equation (Eq. (1)).

$$\text{TotalCamobilizationrate}(\text{nmold}^{-1}) = \frac{\text{Ca}[\text{nmol}]_{\text{day14}} - \text{Ca}[\text{nmol}]_{\text{day0}}}{14[\text{days}]} \quad (1)$$

where $\text{Ca}[\text{nmol}]$ represents the amount of Ca at the end (day 14) and the beginning (day 0) of the experiment. The net Ca solubilization rate (nmol d^{-1}) from calcareous parent materials was estimated as the

difference between the total Ca mobilization rate (biotic + abiotic) and the release rate determined in the sterile control experiment as follows:

$$\text{NetCasolubilizationrate}(\text{nmold}^{-1}) = \text{totalCamobilizationrate}(\text{nmold}^{-1}) - \text{Careleaseratefromsterilecontrol}(\text{nmold}^{-1}) \quad (2)$$

We consider this a net rate because we did not correct for microbial Ca uptake. The net Ca solubilization rates were divided by the corresponding amount of calcareous parent material utilized as well as by the respective surface area of the weathered parent material ($\text{m}^2 \text{g}^{-1}$) to result in a final rate expressed as $\text{nmol m}^{-2} \text{d}^{-1}$.

In addition, we determined the gross P solubilization rates, i.e., the total amount of P released from calcareous parent materials, based on the Ca and P content of the parent materials and the net Ca solubilization rates, as follows:

The gross P solubilization rates were divided by the corresponding amount of calcareous parent material as well as by the respective surface area of the weathered parent material ($\text{m}^2 \text{g}^{-1}$) to result in a rate expressed as $\text{nmol m}^{-2} \text{d}^{-1}$. Both the net Ca and the gross P solubilization rates ($\text{nmol m}^{-2} \text{d}^{-1}$) are given per unit area of parent material ($\text{m}^2 \text{g}^{-1}$). P is generally solubilized when P-containing calcareous rock weathers and the gross solubilization rates of Ca and P during weathering reflect the Ca:P ratio of the rock (Hartmann et al., 2014). Here we followed Gardner (1990) who suggested to use the export of dissolved Si as a weathering index to estimate the rate of P release due to chemical weathering by means of the P:Si loss ratio in saprolite.

To check if variables were normally distributed, the Shapiro-Wilk test was performed ($p > 0.05$). Further, all data sets were tested for equality of variance using Levene’s test. When variances were not significantly different between groups, analysis of variance (one-way ANOVA) was used to test for differences between soil properties and net Ca solubilization rates. Differences in Ca and P solubilization rates between the two soil depths were analyzed by *t*-test followed by post-hoc Tukey HDS ($p < 0.05$). For unequal numbers of observation with equal variance, the parametric Holm-Sidak post hoc test was used (siliceous vs. calcareous parent materials). Linear regression analysis was used to test for a relationship between the amounts of Ca and P in solution. Tests for correlations were made using Spearman correlation analysis. All statistical analysis was performed using SigmaPlot (version 13.0, Systat Software, San Jose, California, USA).

3. Results

3.1. Net Ca solubilization from weathered calcareous parent material

The amounts of dissolved Ca increased during the two-week period only in the experiment with the addition of glucose, but not in the experiment without addition of glucose, as shown in Table S1. Moreover, we found that the dissolved Ca concentrations were up to 79.4% higher in the biotic experiment compared to the abiotic experiment (sterile conditions). Rates of Ca solubilization normalized to the surface area of the weathered calcareous parent material differed significantly among the two soils and the two soil horizons (Fig. 1). The net Ca solubilization rate from the two different parent materials incubated in soil water extracts and glucose ranged between 8.8 (± 7.7) and 511.1 (± 25.4) $\text{nmol m}^{-2} \text{d}^{-1}$ over the two-week period. Dolomite showed

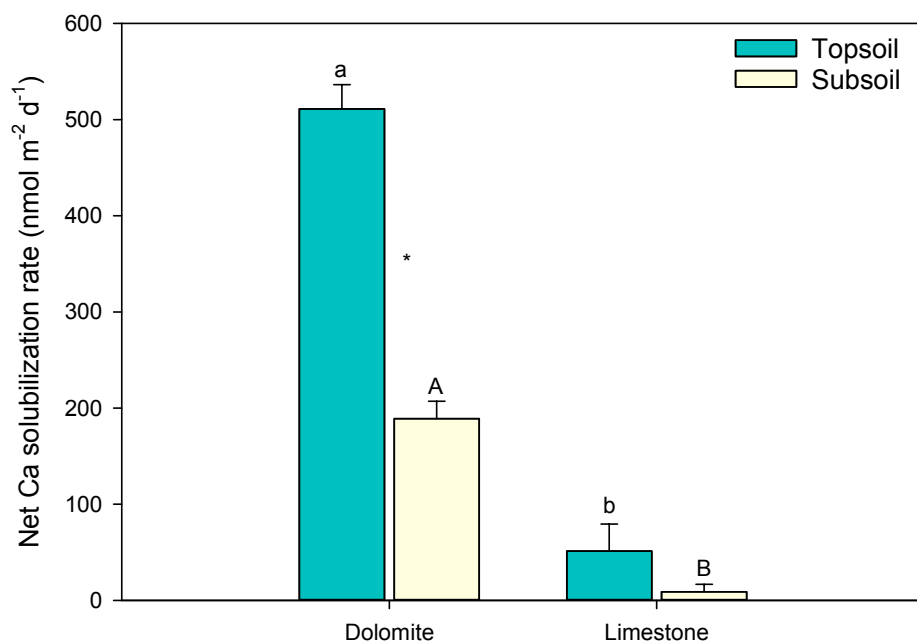


Fig. 1. Net Ca solubilization rates from calcareous rocks incubated in soil extracts from two forest soils with glucose. The rates were normalized according to the specific surface area of the rocks and computed over 14 days of incubation. Soils and rocks were sampled at two different depths of two forest soils developed on dolomite (topsoil: 4–9 cm and subsoil: 22–37 cm) or on limestone (topsoil: 11–18 cm and subsoil: 42–60 cm). Bars show means and error bars indicate standard deviations ($n = 3$). Different letters indicate significant differences tested separately for the two soil depths by one-way ANOVA followed by post-hoc Tukey HDS ($p < 0.05$). Stars indicate significant differences between the two depths of each soil, tested by t -test followed by post-hoc Tukey HDS ($p < 0.05$).

higher net Ca solubilization rates in comparison to limestone (Fig. 1, $p < 0.05$). At the dolomite site, the net Ca solubilization rates in the upper soil horizon were significantly higher than in the lower soil horizon (+63%; $p < 0.001$), while no statistically significant difference in the net Ca solubilization rates was observed between the upper and the lower soil horizon in incubations with limestone (Fig. 1). At the dolomite site, the extracts from the topsoil showed the highest pH decrease (from 7.8 to 6.9), in particular during the first three days of the incubation. The pH in the extracts from the subsoil at both sites decreased much less and, after three days, a slight increase in pH was registered (Table 5). The amounts of Ca were negatively related to the amounts of P in solution, with the best-fitting, linear model for the dolomite soil (topsoil $R^2 = 0.87$; subsoil $R^2 = 0.40$, $p < 0.05$).

3.2. Gross P solubilization from weathered calcareous parent material

During the incubation experiments, we did not observe any net P solubilization but rather P immobilization, as indicated by a steady decline in the concentration of phosphate over the two-week period (Table S2). However, we determined the gross P solubilization rates from the P and Ca content of the parent materials and the net Ca solubilisation rate. Gross P solubilization normalized to the surface area of the weathered calcareous parent material ranged from $0.01 \text{ nmol m}^{-2} \text{ d}^{-1}$ (± 0.00) to $0.17 \text{ nmol m}^{-2} \text{ d}^{-1}$ (± 0.01) (Table 3). Overall, the gross P solubilization rates were significantly higher from dolomite compared to limestone. Moreover, we found that the P concentrations were 12.7% to

Table 3

Gross P solubilization from two calcareous parent materials in two soil horizons determined according to the Ca and P contents of the respective rocks and the Ca solubilization rate computed over 14 days. Mean values and standard deviations (S.D., in parentheses) are shown ($n = 3$). Uppercase and lowercase letters show significant differences tested separately for the two soil depths by one-way ANOVA, followed by post-hoc Tukey HDS ($p < 0.05$).

Site	Soil depth [cm]	Gross P solubilization rate [$\text{nmol m}^{-2} \text{ d}^{-1}$]*
Dolomite	Topsoil (4–9)	$0.17 (\pm 0.01)^a$
	Subsoil (22–37)	$0.05 (\pm 0.00)^A$
Limestone	Topsoil (11–18)	$0.07 (\pm 0.04)^b$
	Subsoil (42–60)	$0.01 (\pm 0.00)^B$

*Computed per g of parent material.

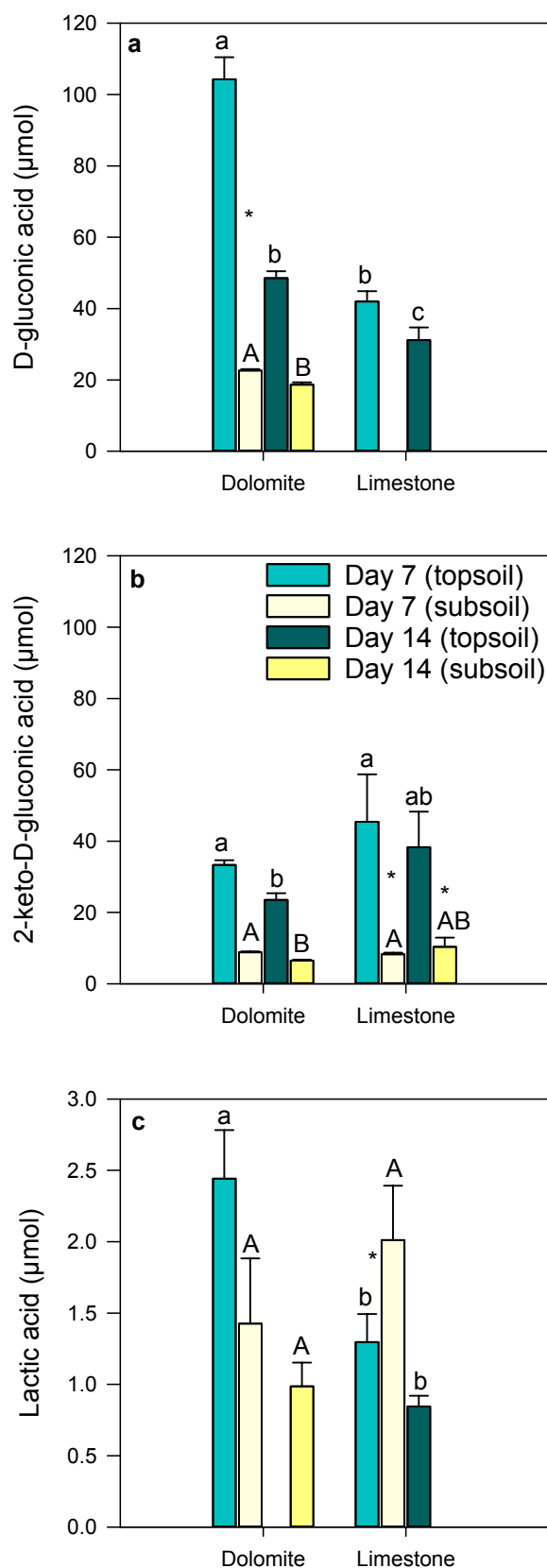
63.4% higher in the biotic experiment compared to the abiotic experiment (sterile conditions).

3.3. Organic acids in soil extracts

Citric and oxalic acids were not detected after 7 and 14 days of incubation, and thus monocarboxylic acids (D-gluconic, 2-keto-D-gluconic and lactic acid) represented 100% of all tested acids at these times. We found that the total amounts of the three measured organic acids were higher in solution with dolomite than with limestone ($p < 0.05$) (Fig. 2). 2-keto-D-gluconic acid prevailed at the limestone soil, whereas D-gluconic and lactic acid dominated at the dolomite soil (Fig. 2). Overall, organic acids decreased significantly from day 7 to day 14 in all soil extracts ($p < 0.05$) (Fig. 2). The sum of organic acids (D-gluconic, 2-keto-D-gluconic and lactic acid) released by microbes was 2.6 to 7.7 times larger in the soil extracts from the topsoil compared to the subsoil at both sites after 14 days of incubation. The amounts of carboxyl groups detected in the extracts from the topsoil after 14 days of incubation had a significant negative relationship with pH ($R^2 = 0.87$ for the dolomite soil and $R^2 = 0.81$ for the limestone soil, $p < 0.05$), whereas in the extracts from the subsoil, the negative relationship between the carboxyl groups and pH occurred only at the dolomite soil ($R^2 = 0.86$, $p < 0.05$).

3.4. Abundance and taxonomic composition of PSB

The relative abundance of culturable PSB ranged from 3.8 % to 24.4 % of all colony-forming bacteria isolated from the two soils and horizons (Fig. 3). Overall, we found that the relative abundance of culturable PSB was significantly higher at the dolomite soil in comparison to the limestone soil for both soil horizons (Fig. 3). Based on the diameter of the halo, by which we discriminated strong versus weak PSB, we found that the dolomite soil harbored on average 28.1% more strong P-solubilizers than the limestone soil in the upper soil horizon (data not shown). In total, 224 PSB colonies were identified by 16S rRNA gene sequence analysis. The sequenced PSB belonged to four phyla (Proteobacteria, Bacteroidetes, Firmicutes and Actinobacteria). Pseudomonadales dominated in both soils and depths, representing almost 80% of all isolates, whereas Enterobacteriales were the second most abundant order and represented, on average, 10% of all PSB OTUs (Fig. 4). Among all sequenced PSB colonies, 32 different OTUs were obtained by



(caption on next column)

Fig. 2. Amounts of D-gluconic (a), 2-keto-D-gluconic (b), and lactic acid (c) calculated based on the concentrations and the volumes of the solutions at day 7 and 14 of the incubation experiment conducted with soil extracts from two forest soils developed on dolomite (topsoil: 4–9 cm and subsoil: 22–37 cm) and limestone (topsoil: 11–18 cm and subsoil: 42–60 cm). Bars represent means and error bars indicate standard deviations ($n = 3$). Different lowercase and uppercase letters show significant differences between soils and soil depths tested separately for day 7 and day 14 by one-way ANOVA followed by post-hoc Tukey HSD ($p < 0.05$). Stars indicate significant differences between two depths of one soil, tested by t -test followed by post-hoc Tukey HSD ($p < 0.05$). Citric and oxalic acids were also investigated but no amounts were detected after 7 and 14 days of incubation. Note the different scales of the y axes.

clustering of the 16S rRNA gene similarity. We found that *Serratia* sp. and *Pseudomonas* sp. were present in all soils. The 16S rRNA gene sequencing revealed seven distinct isolates of *Pseudomonas* at the dolomite soil and only three at the limestone soil. *Erwinia* sp., *Arthrobacter* sp. and *Streptomyces* sp. were found only at the dolomite soil, whereas *Ewingella* sp., *Flavobacterium* sp., *Rahnella* sp. and *Paenibacillus* sp. were found only at the limestone soil. Nonmetric multidimensional scaling (nMDS) analysis revealed that the PSB community at the limestone site was significantly different from the PSB community at the dolomite site ($p < 0.05$).

4. Discussion

4.1. Solubilization of Ca from weathered calcareous rocks

We found that the Ca and P solubilization rates from dolomite were significantly higher than those from limestone (Fig. 1; Table 3), in contrast to our first hypothesis. The most likely reason for this is that the sum of organic acids, as well as the total amounts of carboxyl groups, were significantly higher in the incubation with dolomite than with limestone, in particular during the first week of the incubation when most dissolution of the parent rock occurred (Table 4). Our results agree with Pokrovsky and Schott (2001) who found that dissolution rates of dolomite are strongly promoted by the addition of organic acids. Organic acids can affect solubilization rates of calcareous rock in three ways: (i) by complexation of cations, such as Ca and Mg, (ii) by ligand exchange reactions or (iii) by decreasing the pH of the soil extracts (Hinsinger, 2001; Oburger et al., 2009). Gluconic acid was by far the most abundant organic acid among the ones that were determined, especially in the soil extracts from the topsoil of the dolomite soil, which might be related to the occurrence of Streptomycetales in the dolomite but not in the limestone soil (Fig. 4). Members of the genus *Streptomyces* are able to produce very high amounts of malic and gluconic acids (Jog et al., 2014). Further, the high concentrations of D-gluconic and 2-keto-D-gluconic acids are likely related to the high abundance of *Pseudomonas* and other gram-negative bacteria in both soils (Goldstein, 2007).

In the topsoil, the pH of the soil extracts incubated with dolomite decreased by 1 unit up to a minimum of pH 6.9 during the first week of the experiment (Table 5) probably due to the high amounts of D-gluconic acid released by microbes. Up to 66.64% of the total concentrations of H^+ present in these alkaline soil extracts were probably derived from D-gluconic acid, according to its concentration as well as its pK_a . On the contrary, the pH of the soil extracts incubated with limestone in the topsoil did not decrease significantly during the two-week period with values consistently between 7.9 and 8.1 (Table 5). Thus, pH-mediated solubilization, due to the higher amounts of D-gluconic acid and the related decrease in pH, likely caused the different solubilization rates of the two calcareous parent materials in the upper soil horizon (dolomite \gg limestone).

In the lower soil horizon, the higher Ca solubilization rates from dolomite than from limestone can be explained also by the higher amount of carboxyl groups present in the soil extracts (on average ~ 3.6 times higher in the incubations with dolomite than with limestone).

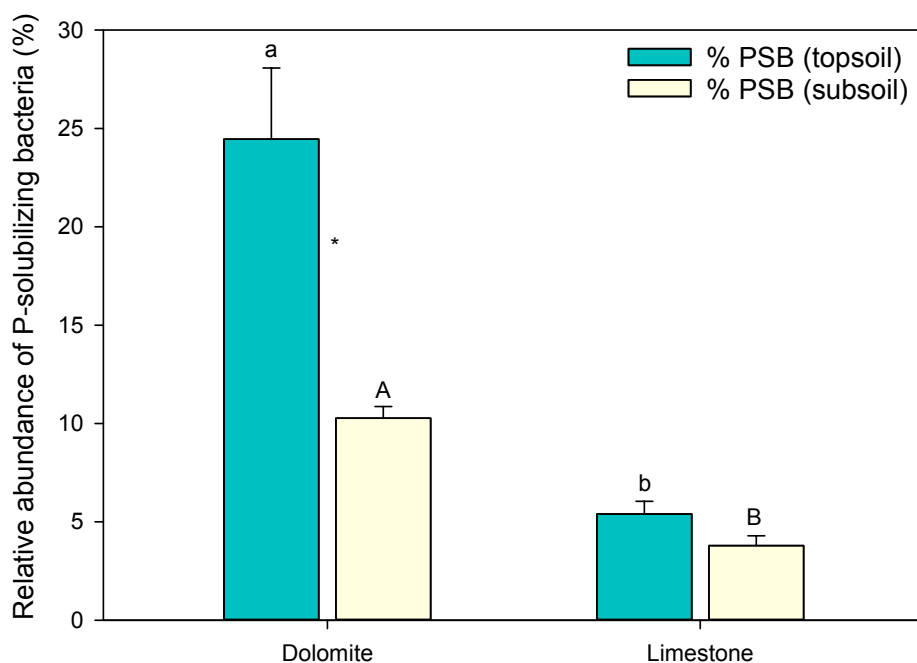


Fig. 3. Relative abundance of culturable P-solubilizing bacteria (PSB) from two forest soils developed on dolomite (topsoil: 4–9 cm and subsoil: 22–37 cm) and limestone (topsoil: 11–18 cm and subsoil: 42–60 cm). Bars represent means and error bars indicate standard deviations ($n = 3$). Different uppercase and lowercase letters indicate significant differences between sites tested separately for each soil depth using one-way ANOVA followed by post-hoc Tukey HSD ($p < 0.05$). Stars indicate significant differences between the two depths of each soil, tested by *t*-test followed by post-hoc Tukey HSD ($p < 0.05$).

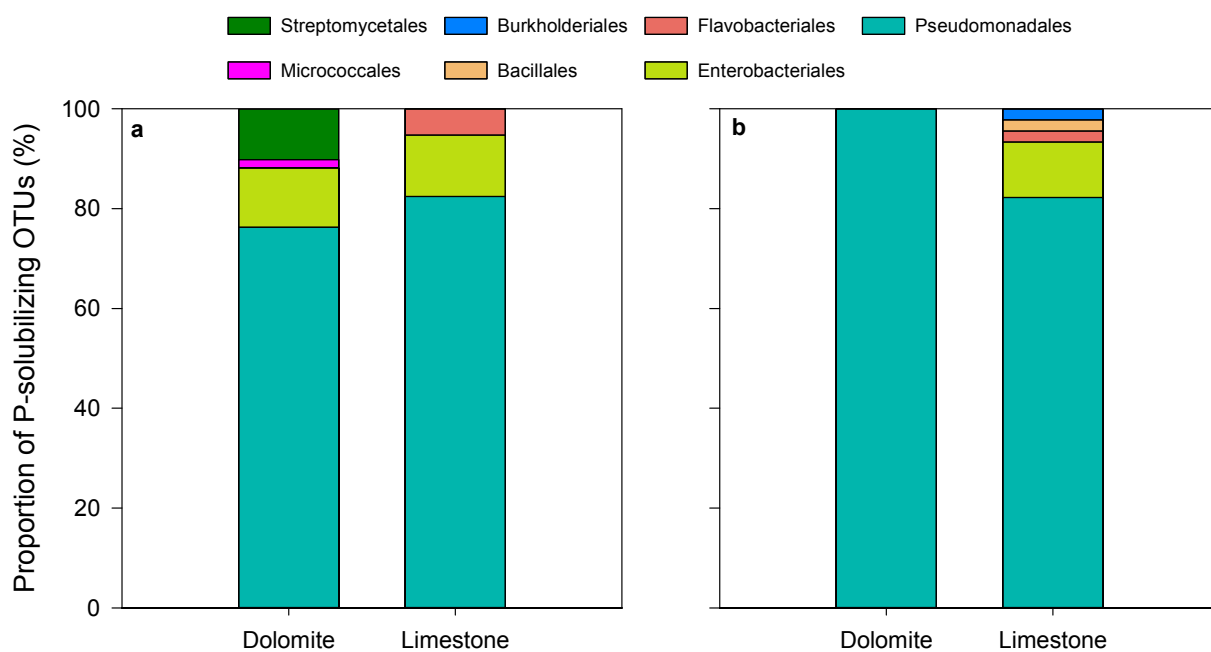


Fig. 4. Relative abundance of different OTUs of P-solubilizing bacteria (PSB) from two forest soils developed on dolomite and limestone in the topsoil (a) and in the subsoil (b). Isolates identified as PSB were grouped into operational taxonomic units (OTU) at 98% cut-off similarity. Taxonomic classification of isolates is shown at the order level.

which, in turn, can likely be related to the higher microbial biomass of the dolomitic soil in comparison to the limestone soil (Table 2). Despite this, in the lower soil horizon, the pH of the soil extracts incubated with dolomite and limestone remained relatively stable (Table 5). This is likely related to the lower microbial biomass in the subsoil in comparison to the topsoil which likely resulted in a smaller rate of proton release.

It is worth mentioning that in this study we worked under laboratory conditions with relatively high temperatures and high organic C availability. This allowed us to determine Ca solubilization by microorganisms from weathered bedrock. However, it has to be taken into account

that temperature in soils tends to be lower than in our incubation experiments. Further, the C availability was high at the beginning of the incubation, which reflects rhizosphere conditions but does not represent conditions in root-free soil. In addition, it needs to be taken into account that the incubation experiment was conducted on a shaker, which is common practice when determining net and gross P mobilization rates (Bünemann, 2015), but likely causes higher solubilization rates than *in situ*.

Comparing the amounts of organic acids in the extracts incubated with calcareous soils to a previous study on siliceous soils (Pastore et al., 2020b) we found they were significantly higher than those measured in

Table 4

Sum of carboxyl groups released by microbes in soil extracts incubated with two different calcareous parent materials (dolomite and limestone). Values are shown for day 7 and day 14 of the incubation.

Site	Soil depth [cm]	Sum of carboxyl groups [μmol] *	
		Day 7	Day 14
Dolomite	Topsoil (4–9)	140.1	48.1
	Subsoil (22–37)	32.9	26.2
Limestone	Topsoil (11–18)	88.3	70.1
	Subsoil (42–60)	9.6	6.9

* Computed for the three measured organic acids.

the incubations with silicates in the topsoil (+75.6%; $p < 0.05$), whereas no significant differences were observed in the extracts from the subsoil (Fig. S1). In particular, we found that the concentrations of D-gluconic and 2-keto-D-gluconic acids in the incubation experiment with the calcareous soils were 71% and 62%, respectively, higher than in the incubation experiment with siliceous soils. The higher concentrations of organic acids in the calcareous soils are likely related to a higher soil microbial biomass (see Table 2) in the calcareous than in the siliceous soils (Pastore et al., 2020b). Our data on the activity of microbial communities in alkaline soils is in accordance with a previous finding by Tyler and Ström (1995) who found that calcicole plants, which mainly establish on calcareous soils, release more organic acids in comparison to calcifuge plants, which mainly establish on silicate soils. However, to date, the evidence for a higher release of organic acids in alkaline soils compared to siliceous soils is still very limited (see also Syers et al., 1967; López-Bucio et al., 2000). Altogether, our study suggests that the Ca solubilisation rate from the two calcareous rocks was strongly affected by pH and the organic acid concentration which, in turn, likely resulted from a difference in microbial biomass between the two soils.

4.2. Solubilization of P from weathered calcareous rocks

The stoichiometrically-derived gross P solubilization rates from dolomite were significantly higher than the ones from limestone although the latter carried almost 6.7 times more P than dolomite (Table 1). The reason for this is the higher Ca solubilization rates from dolomite. Calcium is released from carbonates, while P is mainly released from primary P-minerals (apatites) and, secondary, from P adsorbed to minerals. The assumption made here is that Ca and P are solubilized in the same proportion as they are found in the weathered bedrock. In the long-term, the ratio of gross Ca to gross P solubilization during weathering must reflect the ratio of Ca:P in the rock. However, for the short-term, this assumption might have led to an overestimation of P solubilization as the solubility of apatite is low compared to carbonates (see also Guidry and Mackenzie, 2003; Mair et al., 2017) and apatite is not homogeneously distributed in calcareous rock. However, it could also be that P was preferentially solubilized by microorganisms, as observed in a recent study on solubilisation of P from siliceous saprolite (Spohn et al., 2020).

Table 5

pH values of the soil extracts incubated with two calcareous parent materials in the experiment with and without addition of glucose.

Site	Soil depth [cm]	Experiment with glucose				Experiment without glucose			
		pH				pH			
		DAY 0	DAY 3	DAY 7	DAY 14	DAY 0	DAY 3	DAY 7	DAY 14
Dolomite	4–9	7.8 (± 0.11)	6.9 (± 0.17)	7.8 (± 0.07)	8.1 (± 0.05)	7.9 (± 0.01)	7.9 (± 0.03)	8.0 (± 0.05)	8.2 (± 0.06)
	22–37	7.9 (± 0.04)	7.9 (± 0.07)	8.1 (± 0.09)	8.3 (± 0.05)	7.9 (± 0.11)	8.0 (± 0.06)	8.1 (± 0.07)	8.2 (± 0.08)
	11–18	8.0 (± 0.01)	7.9 (± 0.02)	8.1 (± 0.03)	8.1 (± 0.05)	7.9 (± 0.08)	7.9 (± 0.01)	8.1 (± 0.01)	8.0 (± 0.08)
Limestone	42–60	8.0 (± 0.01)	7.9 (± 0.03)	8.0 (± 0.03)	8.1 (± 0.06)	7.8 (± 0.05)	7.9 (± 0.04)	8.0 (± 0.01)	8.0 (± 0.06)

When the data on gross P solubilization rates were compared to those obtained from a previous study (Pastore et al., 2020b) we found that significantly less P was released from carbonates than from silicates (Fig. S3a) despite the fact that the net Si solubilization rates from silicates were lower than the net Ca solubilization rates from carbonates. The reason for this is that silicates carried on average 12 times more P than the carbonates (2.25 g P kg^{-1} in silicates and 0.19 g P kg^{-1} in carbonates). Thus, to determine the effect of soil extracts on gross P solubilization under the same conditions, we recalculated the P release assuming that the carbonates would have the same P content as silicates. The results show that the “potential” of microbes to solubilize P from calcareous rocks was 3.2 times higher than silicate rocks in the topsoil (Fig. S3b; $p < 0.05$) and ~ 1.6 times higher in the subsoil. Taken together, our results suggest that high rates of mineral dissolution can compensate for low mineral P content.

4.3. Abundance of PSB

The higher abundance of PSB in the soil derived from dolomite fits well with the high Ca and P solubilization rates at this site, indicating that the abundance of PSB is related to mobilization of Ca and P from the weathered calcareous parent materials. We found that the relative abundance of culturable PSB in the two mineral soils ranged from 3.8 % in the limestone soil to 24.4 % in the dolomite soil (Fig. 3). Previous studies pointed out that the relative abundance of PSB can constitute up to 53% of total number of culturable bacteria in soils (Browne et al., 2009; Zheng et al., 2019). The higher relative abundance of PSB at the dolomite site (P-poor soil) in comparison to the limestone site (P-rich soil) may be due to environmental pressures favoring organisms that can strongly mobilize P when P is limiting (Nicolitch et al., 2016; Spohn et al., 2020). On the contrary, the lower occurrence of PSB in the soil derived from limestone might be due to a lower microbial investment into organic acids when P is easily available (Jones et al., 2009; Forstner et al., 2019). This would also explain why the dolomite soil harbored stronger P-solubilizers in comparison to the limestone soil. We found that Pseudomonadales and Enterobacteriales, known to be strong P solubilizers (Rodríguez et al., 2007; Nassal et al., 2018), dominated in both soils and depths (Fig. 4). Also, our findings agree with Liu et al. (2015) who reported that Pseudomonadales and Bacillales are the most abundant PSB strains in calcareous soils.

We found that the relative abundance of culturable PSB was significantly higher in calcareous than in siliceous soils studied previously (see Pastore et al., 2020b; Fig. S2; $p < 0.05$). This is in accordance with Zheng et al. (2019) who reported that the abundance of PSB increases with soil pH. In addition, Rodríguez-Navarro et al. (2012) found that calcitic substrates offer a higher affinity for bacterial attachment than silicate substrates, thereby fostering a higher bacterial growth and metabolic activity. The higher relative abundance of PSB can also explain the higher gross P solubilization rates in calcareous soils in comparison to siliceous soils in both soil depths (Fig. S3b). Further, nonmetric multi-dimensional scaling analyses (nMDS) revealed that the PSB communities at the calcareous soils were significantly different from the PSB communities found at the siliceous soils studied in Pastore

et al. (2020b; Fig. S5, $p < 0.05$). Bacillales and Burkholderiales dominated in siliceous soils, whereas Pseudomonadales, and to a much lesser extent Enterobacteriales, were the dominant orders in calcareous soils. Our data show that the genus *Pseudomonas*, which is reputed to have superior P solubilization ability among PSB (Goldstein, 1995; Browne et al., 2009), was by far predominant in calcareous soils in comparison to siliceous soils where it only occurred at the P-poor site. This finding suggests that the higher occurrence of Pseudomonadales might be related to the low P availability in alkaline soils. Taken together, this study suggests that the dolomite site (P-poor soil) had a higher relative abundance of PSB in comparison to the limestone site (P-rich soil) which indicates that there is likely a selective pressure in P-poor soils towards a higher abundance of PSB.

5. Conclusions

We found that the weathering of calcareous rocks was strongly affected by the activity of soil microorganisms. Soil microorganisms incubated with weathered calcareous bedrocks produced large amounts of monocarboxylic acids (mainly D-gluconic acid and, to a lesser extent, 2-keto-D-gluconic acid). Di- and tri-carboxylic acids were not found among the organic acids tested. The higher microbial P solubilization from dolomite in comparison to limestone was mainly caused by the high amounts of D-gluconic acid, especially in the upper soil horizon. Stoichiometrically-derived gross P solubilization rates were significantly higher at the P-poor soil (dolomite) compared to the P-rich soil (limestone). The high Ca and P solubilization rates are in agreement with the higher relative abundance of PSB in the dolomite soil in comparison to the limestone soil. Overall, Pseudomonadales and Enterobacteriales were the two most widely occurring PSB OTUs across the two mineral soils. The higher occurrence of Pseudomonadales, which are reputed to strongly solubilize P compared to other bacteria, might be related to the low solubility of calcareous rocks in alkaline soils. In conclusion, this study shows that the rates of Ca solubilization from weathered calcareous parent materials are related to the activity of soil microorganisms.

Declaration of Competing Interest

The authors declare that they have no known competing financial interests or personal relationships that could have appeared to influence the work reported in this paper.

Acknowledgements

This research was funded by the German Research Foundation (DFG) as part of the project SP 1389/4-2 of the priority program "Ecosystem nutrition: Forest strategies for limited phosphorus resources". We are particularly obliged to Jörg Prietzel of Technische Universität München (TUM) for having provided us with the soil samples and calcareous parent materials. We are grateful to Michaela Hochholzer and Andrea Kirpal of the Keylab for Genomics and Bioinformatics for the molecular biology part. We thank Katerina Diakova for her helpful comments on a previous version of the manuscript. The authors gratefully acknowledge Uwe Hell, Karin Söllner, Renate Krauß and Anita Gößner for assistance provided in the laboratory. Finally, we thank members of the Laboratory for Analytical Chemistry (BayCEER) for the chemical analyses.

Appendix A. Supplementary data

Supplementary data to this article can be found online at <https://doi.org/10.1016/j.geoderma.2021.115408>.

References

- Arvin, L.J., Riebe, C.S., Aciego, S.M., Blakowski, M.A., 2017. Global patterns of dust and bedrock nutrient supply to montane ecosystems. *Am. Assoc. Adv. Sci.* 3, eaa01588. <https://doi.org/10.1126/sciadv.aao1588>.
- Banfield, J.F., Barker, W.W., Welch, S.A., Taunton, A., 1999. Biological impact on mineral dissolution: application of the lichen model to understanding mineral weathering in the rhizosphere. *PNAS* 96 (7), 3404–3411. <https://doi.org/10.1073/pnas.96.7.3404>.
- Bengtsson, Å., Sjöberg, S., 2009. Surface complexation and proton-promoted dissolution in aqueous apatite systems. *Pure Appl. Chem.* 81 (9), 1569–1584. <https://doi.org/10.1351/PAC-CON-08-10-02>.
- Bisutti, I., Hilke, I., Raessler, M., 2004. Determination of total organic carbon - an overview of current methods. *Trends Anal. Chem.* 23 (10-11), 716–726. <https://doi.org/10.1016/j.trac.2004.09.003>.
- Brookes, P.C., Powlson, D.S., Jenkinson, D.S., 1982. Measurement of microbial biomass phosphorus in soil. *Soil Biol. Biochem.* 14 (4), 319–329. [https://doi.org/10.1016/0038-0717\(82\)90001-3](https://doi.org/10.1016/0038-0717(82)90001-3).
- Browne, P., Rice, O., Miller, S. H., Burke, J., Dowling, D. N., Morrissey, J. P., O'Gara, F., 2009. Superior inorganic phosphate solubilization is linked to phylogeny within the Pseudomonas fluorescens complex. *Appl. Soil Ecol.* 43, 131–138. <https://doi.org/10.1016/j.apsoil.2009.06.010>.
- Brucker, E., Kernchen, S., Spohn, M., 2020. Release of phosphorus and silicon from minerals by soil microorganisms depends on the availability of organic carbon. *Soil Biol. Biochem.* 143, 107737. <https://doi.org/10.1016/j.soilbio.2020.107737>.
- Bünemann, E.K., 2015. Assessment of gross and net mineralization rates of soil organic phosphorus—a review. *Soil Biol. Biochem.* 89, 82–98. <https://doi.org/10.1016/j.soilbio.2015.06.026>.
- Christophel, D., Spengler, S., Schmidt, B., Ewald, J., Prietzel, J., 2013. Customary close-to-nature forest management has considerably decreased organic carbon and nitrogen stocks in soils of the Bavarian Limestone Alps. *For. Ecol. Manage.* 305, 167–176. <https://doi.org/10.1016/j.foreco.2013.05.054>.
- Dreybrodt, W., Lauckner, J., Zaihua, L., Svensson, U., Buhmann, D., 1996. The kinetics of the reaction $\text{CO}_2 + \text{H}_2\text{O} \rightarrow \text{H}^+ + \text{HCO}_3^-$ as one of the rate limiting steps for the dissolution of calcite in the system $\text{H}_2\text{O}-\text{CO}_2-\text{CaCO}_3$. *Geochim. Cosmochim. Acta* 60 (18), 3375–3381. [https://doi.org/10.1016/0016-7037\(96\)00181-0](https://doi.org/10.1016/0016-7037(96)00181-0).
- Fairbridge, R.W., Bissell, H.J., Chilingar, G.V., 1967. Developments in sedimentology. *Carbonate Rocks* 9B, 1–21. [https://doi.org/10.1016/S0070-4571\(08\)71028-8](https://doi.org/10.1016/S0070-4571(08)71028-8).
- Finlay, R., Mahmood, S., Rosenstock, N., Bolou-Bi, E., Köhler, S., Fahad, Z., Rosling, A., Wallander, H., Belyazid, S., Bishop, K., Lian, B., 2019. Biological weathering and its consequences at different spatial levels – from nanoscale to global scale. *Biogeosci. Discuss.* 1–43. <https://doi.org/10.5194/bg-2019-41>.
- Forstner, S.-J., Wechsberger, V., Stecher, S., Müller, S., Keiblinger, K.M., Wanek, W., Schleppl, P., Gundersen, P., Tatzber, M., Gerzabek, M.H., Zechmeister-Boltenstern, S., 2019. Resistant soil microbial communities show signs of increasing phosphorus limitation in two temperate forests after long-term nitrogen addition. *Front. Forests Global Change* 2. <https://doi.org/10.3389/ffgc.2019.0007310.3389/ffgc.2019.00073.s00110.3389/ffgc.2019.00073.s00210.3389/ffgc.2019.00073.s00310.3389/ffgc.2019.00073.s00410.3389/ffgc.2019.00073.s00510.3389/ffgc.2019.00073.s006>.
- Gardner, L.R., 1990. The role of rock weathering in the phosphorus budget of terrestrial watersheds. *Biogeochemistry* 11 (2), 97–110.
- Goldstein, A.H., 1995. Recent progress in understanding the molecular genetics and biochemistry of calcium phosphate solubilization by gram negative bacteria. *Biol. Agric. Hortic.* 12 (2), 185–193. <https://doi.org/10.1080/01448765.1995.9754736>.
- Goldstein, A.H., 2007. In: *Developments in Plant and Soil Sciences First International Meeting on Microbial Phosphate Solubilization*. Springer Netherlands, Dordrecht, pp. 91–96.
- Guidry, M.W., Mackenzie, F.T., 2003. Experimental study of igneous and sedimentary apatite dissolution: control of pH, distance from equilibrium, and temperature on dissolution rates. *Geochim. Cosmochim. Acta* 67 (16), 2949–2963. [https://doi.org/10.1016/S0016-7037\(03\)00265-5](https://doi.org/10.1016/S0016-7037(03)00265-5).
- Hartmann, J., Moosdorf, N., Lauerwald, R., Hinderer, M., West, A.J., 2014. Global chemical weathering and associated P-release - the role of lithology, temperature and soil properties. *Chem. Geol.* 363, 145–163. <https://doi.org/10.1016/j.chemgeo.2013.10.025>.
- Hinsinger, P., 2001. Bioavailability of soil inorganic P in the rhizosphere as affected by root induced chemical changes: a review. *Plant Soil* 237, 173–195. <https://doi.org/10.1023/A:1013351617532>.
- Jenkinson, D.S., Brookes, P.C., Powlson, D.S., 2004. Measuring soil microbial biomass. *Soil Biol. Biochem.* 36, 5–7. <https://doi.org/10.1016/j.soilbio.2003.10.002>.
- Jog, R., Pandya, M., Nareshkumar, G., Rajkumar, S., 2014. Mechanism of phosphate solubilization and antifungal activity of *Streptomyces* spp. isolated from wheat roots and rhizosphere and their application in improving plant growth. *Microbiology* 160, 778–788. <https://doi.org/10.1099/mic.0.074146-0>.
- Jones, D.L., Nguyen, C., Finlay, R.D., 2009. Carbon flow in the rhizosphere: carbon trading at the soil-root interface. *Plant Soil* 321 (1-2), 5–33. <https://doi.org/10.1007/s11104-009-9925-0>.
- Joergensen, R.G., 1996. The fumigation-extraction method to estimate soil microbial biomass: calibration of the K_{EC} value. *Soil Biol. Biochem.* 28 (1), 25–31. [https://doi.org/10.1016/0038-0717\(95\)00102-6](https://doi.org/10.1016/0038-0717(95)00102-6).
- Kaufmann, G., Dreybrodt, W., 2007. Calcite dissolution kinetics in the system $\text{CaCO}_3-\text{H}_2\text{O}-\text{CO}_2$ at high undersaturation. *Geochim. Cosmochim. Acta* 71 (6), 1398–1410. <https://doi.org/10.1016/j.gca.2006.10.024>.

- Katoh, K., Standley, D.M., 2013. MAFFT multiple sequence alignment software version 7: improvements in performance and usability. *Mol. Biol. Evol.* 30 (4), 772–780. <https://doi.org/10.1093/molbev/mst010>.
- Khan, A.A., Jilani, G., Akhtar, M.S., Naqvi, S.M.S., Rasheed, M., 2009. Phosphorus Solubilizing Bacteria: occurrence, mechanisms and their role in crop production. *J. Agric. Biol. Sci.* 1, 48–58.
- Lindsay, W.L., 1979. *Chemical Equilibria in Soils*. John Wiley and Sons, New York, pp. 1–449.
- Liu, Z., Yuan, D., Dreybrodt, W., 2005. Comparative study of dissolution rate-determining mechanisms of limestone and dolomite. *Environ. Geol.* 49 (2), 274–279. <https://doi.org/10.1007/s00254-005-0086-z>.
- Liu, Z., Li, Y.C., Zhang, S., Fu, Y., Fan, X., Patel, J.S., Zhang, M., 2015. Characterization of phosphate-solubilizing bacteria isolated from calcareous soils. *Appl. Soil Ecol.* 96, 217–224. <https://doi.org/10.1016/j.apsoil.2015.08.003>.
- López-Bucio, J., Nieto-Jacobo, M.F., Ramírez-Rodríguez, V., Herrera-Estrella, L., 2000. Organic acid metabolism in plants: From adaptive physiology to transgenic varieties for cultivation in extreme soils. *Plant Sci.* 160 (1), 1–13. [https://doi.org/10.1016/S0168-9452\(00\)00347-2](https://doi.org/10.1016/S0168-9452(00)00347-2).
- Mair, P., Tropper, P., Harlov, D.E., Manning, C.E., 2017. The solubility of apatite in H₂O, KCl-H₂O, NaCl-H₂O at 800 °C and 1.0 GPa: implications for REE mobility in high-grade saline brines. *Chem. Geol.* 470, 180–192. <https://doi.org/10.1016/j.chemgeo.2017.09.015>.
- Murphy, J., Riley, J.P., 1962. A modified single solution method for the determination of phosphate in natural waters. *Anal. Chim. Acta* 26, 678–681. [https://doi.org/10.1016/S0003-2670\(00\)88444-5](https://doi.org/10.1016/S0003-2670(00)88444-5).
- Napieralski, S., Buss, H., Brantley, S., Lee, S., Xu, H., Roden, E., 2020. Microbial chemolithotrophy mediates oxidative weathering of granitic bedrock. *Proc. Natl. Acad. Sci. U. S. A.* 116 (52), 26394–26401. <https://doi.org/10.1073/pnas.1909970117>.
- Nassal, D., Spohn, M., Eltlbany, N., Jacquiod, S., Smalla, K., Marhan, S., Kandeler, E., 2018. Effects of phosphorus-mobilizing bacteria on tomato growth and soil microbial activity. *Plant Soil* 427 (1–2), 17–37. <https://doi.org/10.1007/s11104-017-3528-y>.
- Nicolitch, O., Colin, Y.M., Turpault, P., Uroz, S., 2016. Soil type determines the distribution of nutrient mobilizing bacterial communities in the rhizosphere of beech trees. *Soil Biol. Biochem.* 103, 429–445. <https://doi.org/10.1016/j.soilbio.2016.09.018>.
- Oburger, E., Kirk, G.J.D., Wenzel, W.W., Puschenreiter, M., Jones, D.L., 2009. Interactive effects of organic acids in the rhizosphere. *Soil Biol. Biochem.* 41 (3), 449–457. <https://doi.org/10.1016/j.soilbio.2008.10.034>.
- Pastore, G., Kaiser, K., Kernchen, S., Spohn, M., 2020a. Microbial release of apatite- and goethite-bound phosphate in acidic forest soils. *Geoderma* 370, 114360. <https://doi.org/10.1016/j.geoderma.2020.114360>.
- Pastore, G., Kernchen, S., Spohn, M., 2020b. Microbial solubilization of silicon and phosphorus from bedrock in relation to abundance of phosphorus-solubilizing bacteria in temperate forest soils. *Soil Biol. Biochem.* 151, 108050. <https://doi.org/10.1016/j.soilbio.2020.108050>.
- Pikovskaya, R.I., 1948. Mobilization of phosphorus in soil in connection with the vital activity of some microbial species. *Mikrobiologiya* 17, 362–370.
- Plante, Alain F., 2007. In: *Soil Microbiology, Ecology and Biochemistry*. Elsevier, pp. 389–432. <https://doi.org/10.1016/B978-0-08-047514-1.50019-6>.
- Pokrovsky, O.S., Schott, J., 2001. Kinetics and mechanism of dolomite dissolution in neutral to alkaline solutions revisited. *Am. J. Sci.* 301, 597–626. <https://doi.org/10.2475/ajs.301.7.597>.
- Porder, S., Ramachandran, S., 2013. The phosphorus concentration of common rocks—a potential driver of ecosystem P status. *Plant Soil* 367 (1–2), 41–55. <https://doi.org/10.1007/s11104-012-1490-2>.
- Prietzl, J., Zimmermann, L., Schubert, A., Christophel, D., 2016. Organic matter losses in German Alps forest soils since the 1970s most likely caused by warming. *Nat. Geosci.* 9 (7), 543–548. <https://doi.org/10.1038/ngeo2732>.
- Prietzl, J., Klysubun, W., Hurtarte, L.C.C., 2021. The fate of calcium in temperate forest soils: a Ca K-edge XANES study. *Biogeochemistry* 152 (2–3), 195–222. <https://doi.org/10.1007/s10533-020-00748-6>.
- Rodríguez, H., Fraga, R., 1999. Phosphate solubilizing bacteria and their role in plant growth promotion. *Biotechnol. Adv.* 17 (4–5), 319–339. [https://doi.org/10.1016/S0734-9750\(99\)00014-2](https://doi.org/10.1016/S0734-9750(99)00014-2).
- Rodríguez, H., Fraga, R., Gonzalez, T., Bashan, Y., 2007. In: *First International Meeting on Microbial Phosphate Solubilization*. Springer Netherlands, Dordrecht, pp. 15–21. https://doi.org/10.1007/978-1-4020-5765-6_2.
- Rodríguez-Navarro, C., Jroundi, F., Schiro, M., Ruiz-Agudo, E., González-Muñoz, M.T., 2012. Influence of substrate mineralogy on bacterial mineralization of calcium carbonate: implications for stone conservation. *Appl. Environ. Microbiol.* 78 (11), 4017–4029. <https://doi.org/10.1128/AEM.07044-11>.
- Ruttenberg, K.C., 2003. The global phosphorus cycle. *Treatise Geochem.* 8, 585–643. <https://doi.org/10.1016/B0-08-043751-6/08153-6>.
- Spohn, M., Zeißig, I., Brucker, E., Widdig, M., Lacher, U., Aburto, F., 2020. Phosphorus solubilization in the rhizosphere in two saprolites with contrasting phosphorus fractions. *Geoderma* 366, 114245. <https://doi.org/10.1016/j.geoderma.2020.114245>.
- Syers, J.K., Birnie, A.C., Mitchell, B.D., 1967. The calcium oxalate content of some lichens growing on limestone. *Lichenologist* 3 (3), 409–414. <https://doi.org/10.1017/S0024282967000416>.
- Tyler, G., Ström, L., 1995. Differing organic-acid exudation pattern explains calcifuge and acidifuge behavior of plants. *Ann. Bot.* 75, 75–78. [https://doi.org/10.1016/S0305-7364\(05\)80011-3](https://doi.org/10.1016/S0305-7364(05)80011-3).
- Taylor, Holly L., Duivesteyn, Isaac J. Kell, Farkas, Juraj, Dietzel, Martin, Dosseto, Anthony, 2019. Technical note: lithium isotopes in dolostone as a palaeo-environmental proxy – an experimental approach. *Clim. Past* 15 (2), 635–646. <https://doi.org/10.5194/cp-15-635-2019>.
- Vance, E.D., Brookes, P.C., Jenkinson, D.S., 1987. An extraction method for measuring soil microbial biomass C. *Soil Biol. Biochem.* 19 (6), 703–707. [https://doi.org/10.1016/0038-0717\(87\)90052-6](https://doi.org/10.1016/0038-0717(87)90052-6).
- Wan, J., Tokunaga, T.K., Williams, K.H., Dong, W., Brown, W., Henderson, A.N., Newman, A.W., Hubbard, S.S., 2019. Predicting sedimentary bedrock subsurface weathering fronts and weathering rates. *Sci. Rep.* 9, 17198. <https://doi.org/10.1038/s41598-019-53205-2>.
- Widdig, M., Schleuss, P.M., Weig, A.R., Guhr, A., Biederman, L.A., Borer, E.T., Crawley, M.J., Kirkman, K.P., Seabloom, E.W., Wragg, P.D., Spohn, M., 2019. Nitrogen and phosphorus additions alter the abundance of phosphorus-solubilizing bacteria and phosphatase activity in grassland soils. *Front. Environ. Sci.* 7, 185. <https://doi.org/10.3389/fenvs.2019.00185>.
- Zaharescu, D.G., Burghilea, C.I., Dontsova, K., Presler, J.K., Hunt, E.A., Domanik, K.J., Amistadi, M.K., Sandhaus, S., Munoz, E.N., Gaddis, E.E., Galey, M., Vaquera-Ibarra, M.O., Palacios-Menendez, M.A., Castrejón-Martínez, R., Roldán-Nicolau, E. C., Li, K., Maier, R.M., Reinhard, C.T., Chorover, J., 2019. Ecosystem-bedrock interaction changes nutrient compartmentalization during early oxidative weathering. *Sci. Rep.* 9, 15006. <https://doi.org/10.1038/s41598-019-51274-x>.
- Zheng, B., Zhang, D., Wang, Y., Hao, X.J., Wadaan, M.A.M., Hozzein, W.N., Peñuelas, J., Zhu, Y.G., Yang, X.R., 2019. Responses to soil pH gradients of inorganic phosphate solubilizing bacteria community. *Sci. Rep.* 9, 25. <https://doi.org/10.1038/s41598-018-37003-w>.